Journal of Applied Polymer Science

Effect of Poly(vinylidene fluoride) Polymorphic Structures on the Crystallization Behavior of Poly(butylene succinate)

Kai Hou, Hai-Mu Ye, Yun-Yang Song, Qiong Zhou
Department of Material Science and Engineering, China University of Petroleum, Beijing 102249, China
Correspondence to: H. -M. Ye (E-mail: yehaimu@cup.edu.cn)

ABSTRACT: The detail information of both α and β form poly(vinylidene fluoride) (PVDF) crystal effect on the crystallization behavior of poly(butylene succinate) (PBS) were systematically studied. The results show that β form PVDF can obviously improve the melt-crystallization temperature of PBS during the nonisothermal crystallization process. Both crystallization time span and spherulitic size of PBS decrease with the increasing amount of β form PVDF, which enhances the primary nucleation of PBS. But α form PVDF shows no nucleating effect on PBS crystallization, exhibiting as almost unchanged T_c values for α form PVDF-blended PBS samples. The intrinsic mechanism for the nucleating effect of β form PVDF on PBS was proposed to be the epitaxial crystallization.
 J. Appl. Polym. Sci. **2014**, *131*, 40991.

KEYWORDS: crystallization; biopolymers & renewable polymers; differential scanning calorimetry (DSC)

Received 21 January 2014; accepted 8 May 2014
DOI: 10.1002/app.40991

INTRODUCTION

Blending one polymer with another is a simple and economical method to obtain required properties of polymer materials for different applications. Among a large amount of two-component systems, blend of two semicrystalline polymers is more complicated but useful, and has provided a novel way to study the crystallization behavior and morphology evolution of polymer science. Till now, much research on crystalline/crystalline blending system has been carried out. Such as poly (butylene succinate) (PBS)/poly(ethylene oxide) (PEO),[1–8] PBS/poly(ethylene adipate) (PEA),[9] poly(vinylidene fluoride) (PVDF)/PBS,[10–15] PVDF/poly(butylene adipate) (PBA),[16–20] poly (L-lactic acid) (PLLA)/PEO,[21–23] etc. Various researches have revealed rather interesting information in confined crystallization,[4–8,11] template crystallization,[12–14] polymorphic structure,[19,20] and so on. However, till now there are few reports on the effect of polymorphic structures of one polymer on crystallization behavior of the other polymer in crystalline/crystalline blend. Polymorphism is a widespread phenomenon in polymers, different crystal forms of one component might show different effect on the other component in the blend. So we carry out study on the crystallization behavior of PBS blended with PVDF by changing the crystal form of PVDF.

PVDF is a widely used semicrystalline polymer, and has been found to exhibit four crystal forms, named as α, β, γ, and δ, respectively.[24,25] Among them, α form is the most common one, which can be easily obtained from the melt-crystallization procedure or solution-cast at high temperature.[26,27] β form PVDF can be prepared through solution-casting at low temperature or by epitaxial crystallization on special substrate.[28–31] The β crystal form has attracted broad interest because of its extensive piezo and pyroelectric applications.[32] PBS is a representative aliphatic polyester and shows well industrial applications.[33] These two semicrystalline polymers show a melting gap about 50°C. The melting points for PVDF and PBS are about 165°C and 114°C, respectively. Therefore, it would be convenient for us to study the effect of PVDF polymorphic structures on the crystallization behavior of PBS in their blend.

In this study, various methods were utilized to investigate the effect of α and β forms PVDF on the crystallization behavior of PBS. Experimental results showed that β form PVDF could serve as nucleating agent for PBS, while α form PVDF could not. The mechanism of β form PVDF nucleating effect on PBS was suggested as the epitaxial crystallization.

EXPERIMENTAL

Materials and Samples Preparation

PBS was synthesized from succinic acid and 1,4-butanediol through a two-step reaction of esterification and polycondensation in molten state, Tetra-*n*-butyl-titanate was used as catalyst during the reaction.[34,35] The product was purified through a dissolution–precipitation way before using. Number-average molecular weight (M_n) and polydispersity index (PDI) of purified product are 4.46×10^4 g/mol and 1.47, respectively. PVDF powder is produced by Arkema Group (France). The product

number of PVDF is labeled as "PVDF−2801", $M_w = 3.8 \times 10^5$ g/mol. The melting point of PVDF measured by differential scanning calorimetry (DSC) is 164.8°C at a heating rate of 10°C/min.

PVDF was blended into PBS matrix through a co-solvent dissolution and evaporation procedure. N,N-dimethyl formamide (DMF) was selected as the solvent. The addition amount of PVDF varied from 1 to 10 wt %, and the solvent evaporating temperature was set at 45°C or 90°C in order to obtain different crystal form PVDF in the blends.

X-ray Diffraction

Wide angle X-ray diffraction (WAXD) measurement for all samples was performed at ambient condition on a PGENERAL XD−3 diffractometer using graphite-filtered Cu $K\alpha$ radiation ($\lambda = 0.154$ nm). The 2θ scanning interval ranged from 10° to 50° with a rate of 2°/min. The scanning step was 0.01°.

Differential Scanning Calorimetry

The nonisothermal and isothermal crystallization behavior of all samples was carried out on a NETZSCH 204 F1 instrument equipped with an intercooler as cooling system. The instrument was calibrated in temperature and in enthalpy with indium standard specimen. Dry argon was used as purge gas at a rate of 50 mL/min.

Polarized Optical Microscope

The spherulitic morphology and crystallization process of different samples were observed on a Leica DM2500P Polarized optical microscope (POM) instrument equipped with a Linkam THMS600 hot stage.

Fourier Transform Infrared Spectroscopy

Fourier transform infrared spectroscopy (FTIR) spectra were recorded on a Nicolet-560 IR spectrometer under the transmission mode by signal averaging over 32 scans at a resolution of 4 cm^{-1} in the wavenumber range of 4000–400 cm^{-1}.

RESULTS AND DISCUSSION

Crystal Structure

Although it had been reported that PBS/PVDF is a miscible crystalline/crystalline blend system,[10] both components could crystallize, respectively, during the melt-cooling procedure or solvent evaporation process.[10,13,14] So it is expected that there were PVDF crystals in as-prepared samples. Figure 1 shows the WAXD diffractograms of neat PBS, neat PVDF, and 5 wt % PVDF-blended PBS samples. When the neat and blended PVDF were prepared by solvent evaporating at 90°C, they both displayed diffraction peaks of 2θ at 17.5° and 18.2°, which are corresponding to the (100) and (020) crystal planes of α form PVDF. When the solution was evaporated at a reduced temperature of 45°C, the neat and blended PVDF displayed a diffraction peak of 2θ at 20.4°, which can be assigned to the characteristic diffraction peak of (200)/(110) planes of β form PVDF. In order to confirm the crystal structure of PVDF with lower content, the casting samples were extracted in chloroform at 25°C to remove most PBS matrix. Figure 2 shows the WAXD diffractiongram of the residuals, it is clear that the crystal forms of PVDF were well controlled. So it is sure that PBS does not change the PVDF crystal modification formation behavior when cast from the DMF solution at different temperature. The diffractograms of neat and blended PBS all exhibit the diffraction peaks of α form PBS. Peaks at 19.4°, 21.7°, 22.5°, and 28.9° are assigned to the (020)/(−111), (021), (110), and (111) crystal planes, respectively. With carefully comparison, a new diffraction peak at 24.9° for PBS can be found only in the β PVDF-blended PBS, which has not been observed in previous literature. The appearance of new diffraction peak might indicate β form PVDF has some special influence on PBS crystallization behavior.

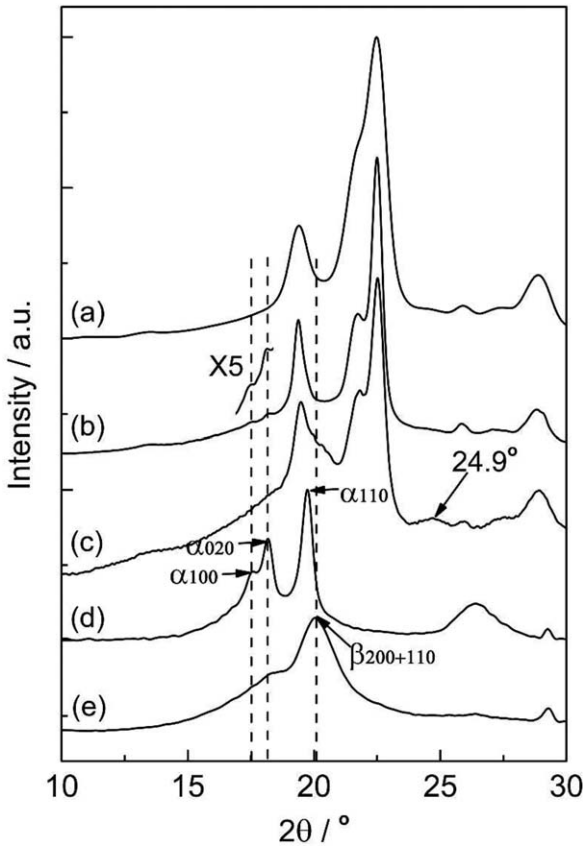

Figure 1. The WAXD diffractograms of (a) neat PBS, 5 wt % PVDF-blended PBS samples obtained by solvent evaporating at (b) 90°C and (c) 45°C, and neat PVDF obtained by solvent evaporating at (d) 90°Cand (e) 45°C.

Nonisothermal Crystallization Behavior

In order to investigate detailed effect of different crystal form PVDF on the crystallization behavior of PBS, both nonisothermal and isothermal crystallization behavior were studied. Figure 3 shows the melt-crystallized DSC curves of neat and blended PBS samples with different addition amounts of β or α form PVDF at a cooling rate of 10°C/min after melting at 135°C for 15 min. The melting condition was selected based on overall consideration for fully melting of PBS but maintaining PVDF crystal form. The crystallization temperature (T_c) of PBS increases with increasing β PVDF. T_c for neat PBS is 75.2°C, and the T_c rises to 86.9°C after adding 10 wt % β PVDF. So β PVDF displays obviously nucleating effect on PBS matrix.

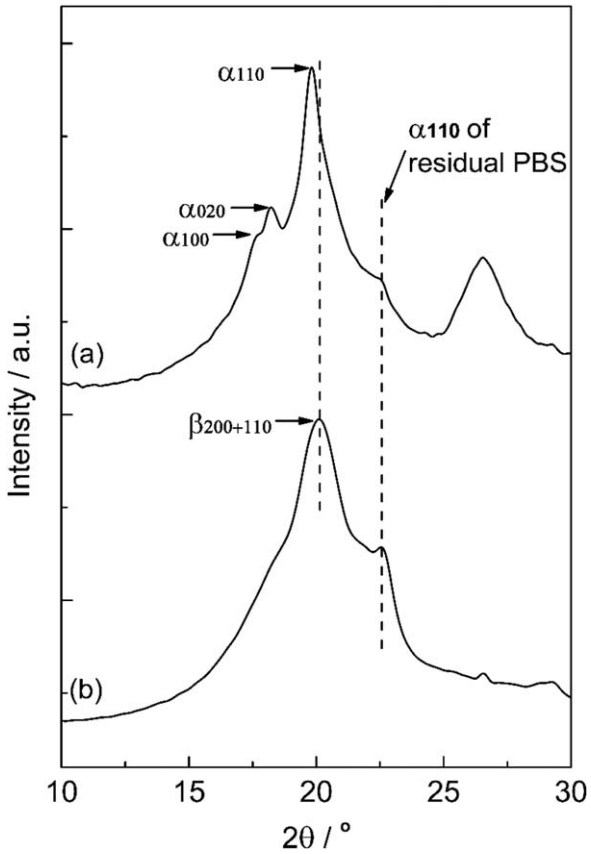

Figure 2. The WAXD diffractiongram of the residuals of (a) 1 wt % α PVDF-blended PBS and (b) 1 wt % β PVDF-blended PBS after being extracted in chloroform at 25°C.

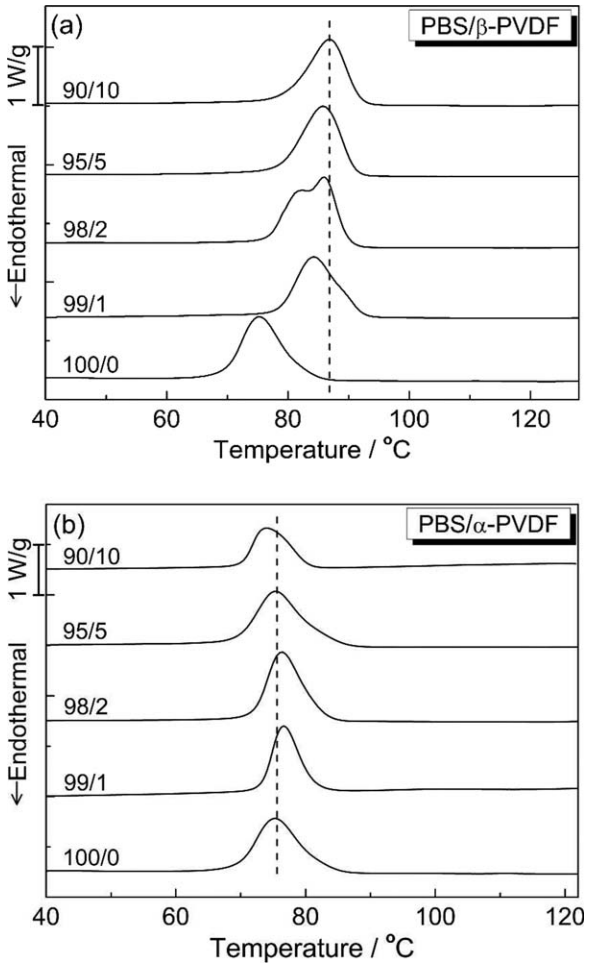

Figure 3. Melt-crystallization curves of PBS with different addition amount of (a) β form PVDF and (b) α form PVDF at a cooling rate of 10°C/min.

Interestingly, a peculiar dual crystallization temperatures behavior was observed for 1 and 2 wt % β PVDF-blended PBS samples. Dual crystallization behavior was sometime observed in some polymer composites because of the coexistence of different nucleation modes.[36,37] In this study, two T_c values of β PVDF-blended PBS were both higher than that of neat PBS, which indicated that the self-nucleation of PBS did not happen although the relevant mechanism have not been figured out yet. Figure 3(b) shows the melt-crystallized DSC curves of α PVDF-blended PBS samples. All T_c values locate around 75.0°C within a temperature shifting of 1.5°C, which indicates that α form PVDF has no acceleration effect on the crystallization of PBS matrix. Similar results have been observed by Nishi et al.[10] and Qiu et al.[12,13] at even higher content of PVDF. Low content of α PVDF almost did not change the T_c value of PBS, and high content of PVDF might depress the T_c because of the dilutive effect.

In Figure 4 neat PBS shows a quite notable exothermal peak during the subsequent heating process after nonisothermal crystallization, marked by an arrow. This phenomenon is usually observed in polyester with slower crystallization rate, such as PLLA[38] and poly(ethylene terephthalate) (PET).[39] Here, the exothermal peak should be connected with the overall performance of recrystallization behavior of less stable crystal structure formed at lower T_c [see Figure 3(a)]. The exothermal peak disappears and double endothermal peaks appear in β PVDF-blended PBS. This melting behavior can be assigned to the melt-recrystallization mechanism[34]: the lower temperature peak

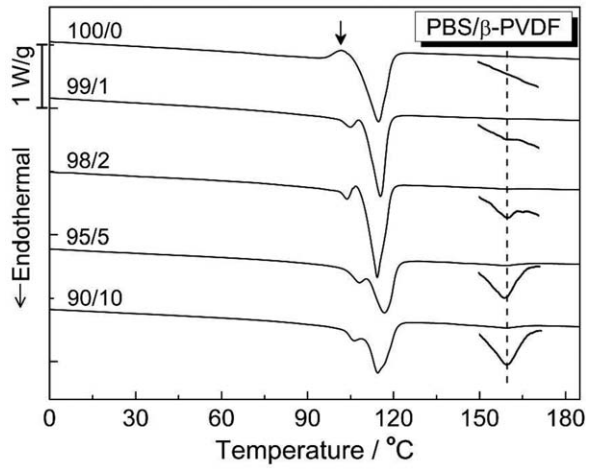

Figure 4. The subsequent heating curves of nonisothermally crystallized PBS samples with different addition amount of β form PVDF at a rate of 10°C/min.

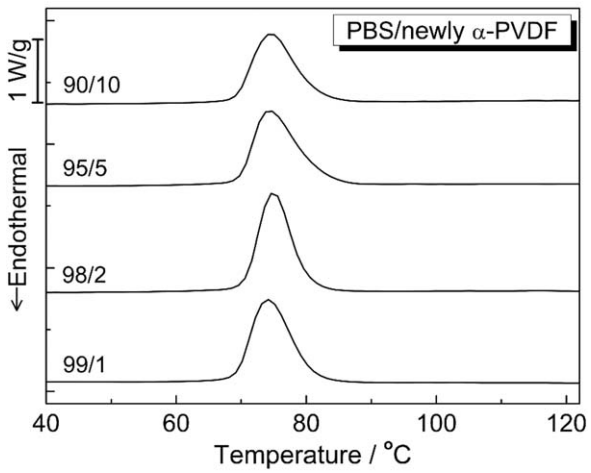

Figure 5. Melt-crystallization curves of PBS with different addition amount of newly formed α form PVDF at a cooling rate of 10°C/min.

is attributed to melting of primary crystal; and the higher one corresponds to melting of recrystallized crystals. In β PVDF-blended PBS, T_c is higher and much perfect crystal structure forms.

To exclude the possible effect originated from the different PVDF dispersion in blended samples when they were obtained at different evaporating temperatures. β PVDF-blended PBS samples were heated to 180°C to transform into newly formed α PVDF-blended PBS samples, then the melt-crystallized DSC curves were measured. T_c values of newly formed samples also all appeared at about 75.0°C, the same as directly prepared α PVDF-blended PBS samples (Figure 5). These results confirm β PVDF can play as effective nucleating agent for PBS, while α PVDF cannot. The nucleating effect of β PVDF on PBS should originate from the crystal structure different from α form.

Isothermal Crystallization Behavior

To further quantify the nucleating ability of PVDF on PBS, isothermal crystallization kinetics of neat and PVDF-blended PBS was investigated. Figure 6(a) shows the DSC curves of different specimens isothermally crystallized at 95°C. Obviously, at such supercooling degree, the crystallization rate of neat PBS is low; it takes longer than 20 min before finishing the total crystallization process. When 1 wt % β form PVDF is introduced, the crystallization time is shortened to around 14 min; and further shortened with more β form PVDF content. The crystallization time span is only about 4 min for 10 wt % β form PVDF-blended PBS, which is just one fifth of neat PBS. The effect of α PVDF on the isothermal crystallization behavior of PBS was also studied, the blended PBS samples showed almost the same behavior as neat PBS, and the data are not shown here for the sake of brevity. The relative crystallinity (X_t) at a given time (t) can be obtained from the integrated area of the DSC curve from $t = 0$ to t divided by the integrated area of the whole exothermal curve. A horizontal line from a point after the crystallization exotherm was used as the baseline for integration, and then the typical sigmoid shape conversion curves of X_t versus t can be attained. Figure 6(b) displays the X_t–t plotting of neat PBS and β PVDF-blended PBS crystallized at 95°C. The process was carefully carried out following the guidelines reported by Lorenzo et al.[40] Then the well-known Avrami equation[41–43] is employed to analyze the overall isothermal melt-crystallization kinetics of PBS. The equation is given as

$$1-X_t=\exp\left(-kt^n\right) \quad (1)$$

where k is the overall rate constant composed of nucleation and growth part, n is the Avrami exponent related to nucleation mechanism (homogeneous or heterogeneous) and growth dimension of crystal. The logarithmic form of equation (1) is written as

$$\lg\left[-\ln\left(1-X_t\right)\right]=\lg k+n\lg t \quad (2)$$

All fits were performed for a relative conversion range encompassing 3–20% to minimize the experimental error.[40] The crystallization parameters n and k are calculated from the slopes and intercepts of fitting lines, respectively, through plotting $\lg[-\ln(1-X_t)]$ versus $\lg t$ [Figure 6(c)]. The correlation coefficients of the plot fit (R^2) for all samples are larger than 0.999. For comparison, n, k, and crystallization half-time ($t_{1/2}$) are summarized in Table I. The calculated Avrami exponents (n) for neat PBS and blended PBS samples fluctuates within the range of 2.8−3.1, suggesting three-dimensional mode with heterogeneous nucleation growth behavior for all samples. The addition of PVDF does not change the spatial growth behavior of PBS. The slightly decrease of n value after adding β form PVDF might indicate the enhancement of heterogeneous nucleation ability. The total crystallization growth rates, reciprocal of crystallization half-time ($t_{1/2}^{-1}$), for the samples with different PVDF contents are drawn in Figure 6(d). The value of $t_{1/2}^{-1}$ for β form PVDF-blended PBS is much larger than that of neat PBS or α form PVDF-blended PBS. The higher $t_{1/2}^{-1}$ value the faster grow rate. $t_{1/2}^{-1}$ values for various α PVDF-blended PBS are approximate to that of PBS, but slightly decrease because of the possible dilutive effect of PVDF or other reason. The $t_{1/2}^{-1}$ values of 5 wt % and 10 wt % β form PVDF-blended PBS samples are about four and seven times of that of neat PBS, respectively. These are quantitative evidences for the better nucleating effect of β form PVDF on PBS. The slowing down of increasing tendency of $t_{1/2}^{-1}$ with more β form PVDF contents is also possibly on account of the dilutive effect of PVDF.

Spherulitic Morphology

Usually, a good nucleating agent provides a surface that reduces the free energy barrier to the primary nucleation, which induces the increase of nucleation density and decrease of spherulitic size. Figure 7 shows the growing and final POM micrographs of neat and PVDF-blended PBS samples isothermally crystallized at 95°C. As the amount of primary nuclei for neat PBS and α PVDF-blended PBS is quite few, the spherulites can finally reach up to around 200 μm before impinging with each other, indicating that α form PVDF has no effect on the primary nucleation of PBS. As to the β form PVDF-blended PBS, much more crystal nuclei are observed at the beginning of crystallization and the size of final spherulite decreases dramatically, which presents directly that β PVDF has greatly enhanced the primary nucleation of PBS during melting crystallization process. These

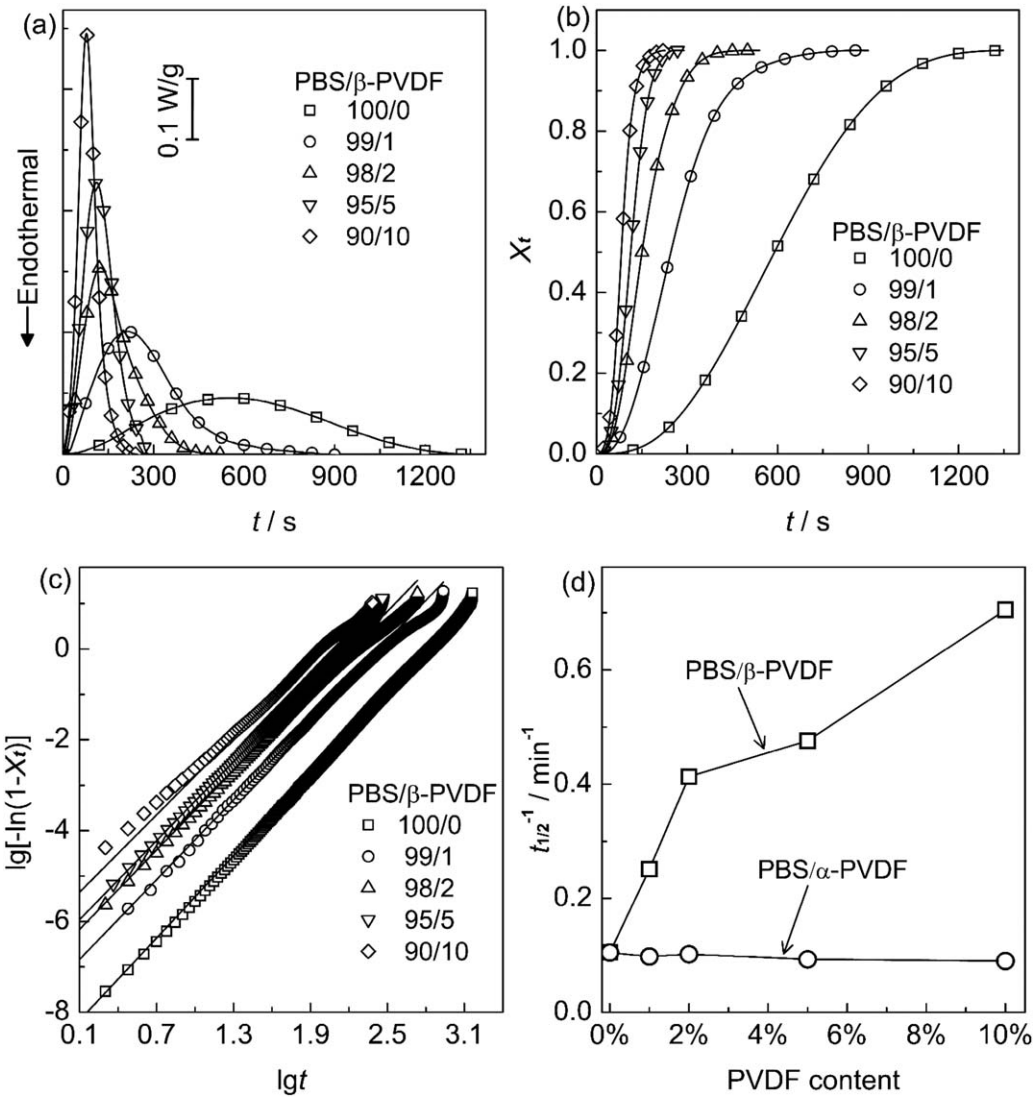

Figure 6. (a) The DSC curves, (b) development of relative crystallinity with crystallization time,) and (c) plotting of $\lg[-\ln(1-X_t)]$ versus $\lg t$ (c) of PBS blended with different contents of β form PVDF isothermally crystallized at 95°C. (d) And the total growth rates ($t_{1/2}^{-1}$) of the samples with different addition amount of PVDF at 95°C.

POM results further prove that β form PVDF can be utilized as an effect nucleating agent for PBS, while α PVDF cannot. This result is in accord with the aforementioned DSC results.

Table I. Avrami Parameters for Neat PBS and PVDF-Blended PBS at 95°C

Samples	n	k (s^{-n})	$t_{1/2}$ (s)
Neat PBS	3.02	3.31×10^{-9}	569
PBS+1wt % β-PVDF	2.93	7.41×10^{-8}	239
PBS+2wt % β-PVDF	2.92	3.39×10^{-7}	145
PBS+5wt % β-PVDF	2.90	5.62×10^{-7}	126
PBS+10wt % β-PVDF	2.84	2.29×10^{-6}	85
PBS+1wt % α-PVDF	3.14	1.19×10^{-9}	612
PBS+2wt % α-PVDF	3.01	3.28×10^{-9}	583
PBS+5wt % α-PVDF	3.17	8.60×10^{-10}	645
PBS+10wt % α-PVDF	3.04	1.81×10^{-9}	666

Discussion

Summarizing the experimental results, polymorphic structures of PVDF have quite different effect on the crystallization behavior of PBS. In this section, we will try to interpret the correspondingly intrinsic nucleating mechanism of β form PVDF on PBS matrix. Until now, two interpretations have been identified as the mechanism of nucleating agent, the chemical and epitaxial nucleation.[44,45] The chemical nucleation is characterized by a chemical reaction between polymer and nucleating agent, resulting in the formation of a new compound that can induce the nucleation of residual polymer chains. However, according to the chemical structure, no possible reaction could occur between PBS and PVDF during the preparation process, thus the chemical nucleation mechanism can be excluded.

In the case of epitaxial nucleation mechanism, the essential requirement is a two-dimensional lattice matching of the two lattice planes in contact between polymer matrix and the

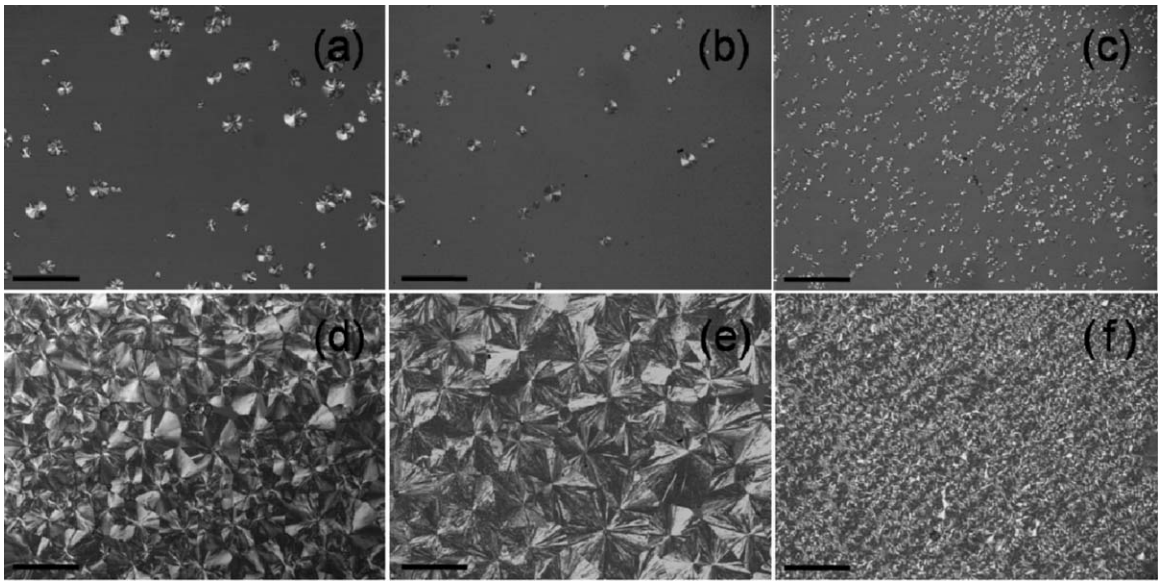

Figure 7. (a,d) The growing and final POM micrographs of neat PBS, (b,e) 10 wt % α form PVDF-blended PBS, and (c,f) 10 wt % β form PVDF-blended PBS isothermally crystallized at 95°C. The scale bar is 200 μm.

nucleator. The unit cell parameters for α form PBS are: $a = 0.523$ nm, $b = 0.908$ nm, $c = 1.079$ nm, $\beta = 123.87°$.[46] The α form PVDF crystal adopts as monoclinic structure with unit cell parameters as: $a = 0.696$ nm, $b = 0.964$ nm, $c = 0.462$ nm, and $\beta = 90°$, and β form PVDF crystal adopts orthorhombic crystal structure with dimensions $a = 0.858$ nm, $b = 0.491$ nm, and $c = 0.256$ nm.[24,25] The length of α form PBS c axis is close to fourfold that of β form PVDF crystal, with a small mismatch degree of 5.1% [eq. (3)], suggesting that the PBS crystals should favor to grow on the surface of (010) planes of β PVDF crystals by an epitaxial mechanism:

$$d_{\mathrm{PBS}}\% = \left|\frac{1.079 - 4\times 0.256}{1.079}\right| \times 100\% = 5.1\% \qquad (3)$$

Another important factor for β form PVDF displaying good nucleating effect on PBS might be because of the successive hydrogen bonds forming between C−H of PVDF and C=O of PBS, as shown in Figure 8. The C−F bonds on the reverse side of C−H bonds play positive effect on the formation of hydrogen bonds due to their strong electron-withdrawing effect. Figure 9 shows the FTIR spectra of neat and blended PBS samples. Bands at 840 and 882 cm^{-1} are the characteristic FTIR absorption bands of β form PVDF crystal and band at 873 cm^{-1} is the characteristic FTIR absorption band of α form PVDF crystal.[47,48] The low shift of C=O vibration absorption band from 1716 to 1712 cm^{-1} indicates that there does exist enhancement interaction on C=O···H−C from C−F structure in β PVDF-blended PBS. Thus, the intrinsic mechanism of

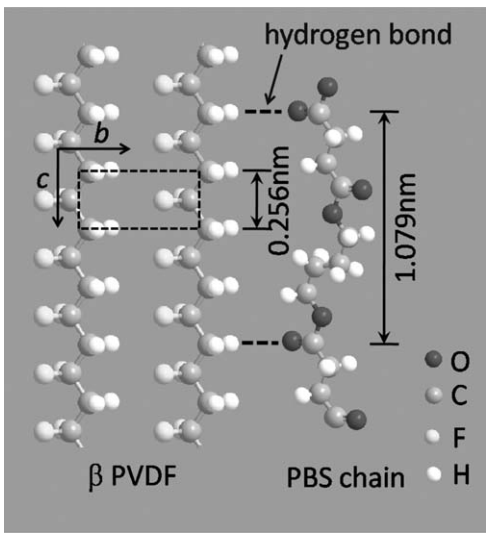

Figure 8. The schematic diagram for the hydrogen bond interaction between β form PVDF crystal and PBS chain.

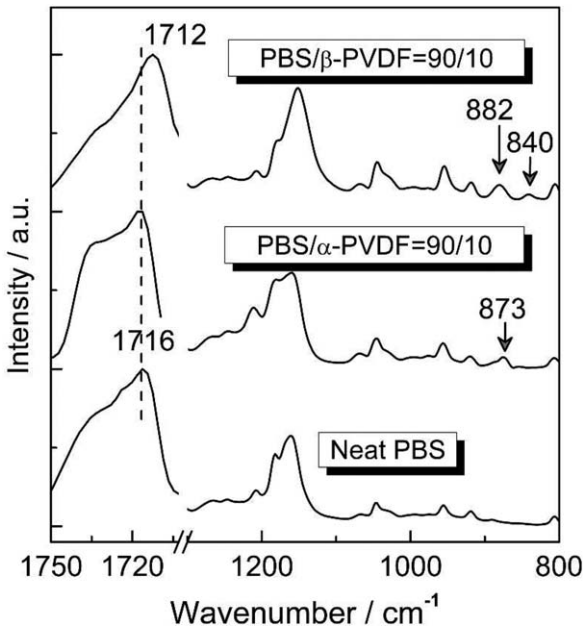

Figure 9. FTIR spectra of neat PBS and 10 wt % PVDF-blended PBS.

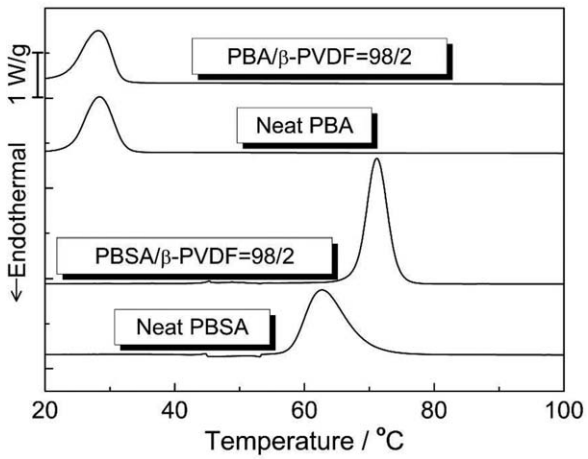

Figure 10. Melt-crystallization DSC curves of neat and 2 wt % β form PVDF-blended polyesters (PBA and PBSA), the cooling rate is 10°C/min.

nucleating effect of β PVDF on PBS can be tentatively discussed as follows. During the crystallization of β form PVDF-blended PBS, mobile PBS chains nearby the β PVDF crystals tend to absorb on the (010) planes because of the strong hydrogen bond interaction; furthermore, the good match along the c axes of unit cell between β form PVDF crystal and PBS crystal reduces the change of conformation entropy of PBS chains during crystallization, which lowers down of crystallization energy barrier and accelerates the crystallization rate.

To gain more experimental verification, β form PVDF-blended PBS-*co*−10 mol%-butylene adipate) (PBSA, $M_n = 2.60 \times 10^4$ g/mol, PDI = 2.13) and β form PVDF-blended poly(butylene adipate) (PBA, $M_n = 5.7 \times 10^4$ g/mol, PDI = 1.82) samples were prepared through the same temperature-controlled solution evaporation process. Figure 10 shows the relative melt-crystallization DSC curves. The T_c value of PBSA increase from 62.7 to 71.1°C after adding 2 wt % β form PVDF, but T_c of PBA is unchanged with the addition of β form PVDF. PBSA was reported to adopt the same crystal structure as PBS by excluding the butylene adipate units as defects from the lamellar core,[49] so it is expected that β form PVDF shows nucleating effect on PBSA. As to PBA, the polymer chains are similar to PBS with two more $-CH_2-$ repeat units in dialkene groups, resulting in longer c axis ($c = 1.420$ nm for α PBA).[50] Because of mismatch of lattice parameters, β PVDF does not accelerate the crystallization ability of PBA. However, Inoue et al. reported that α PVDF could play as nucleating agent for PBA to form α form crystals.[19] The length of α form PBA c axis is closed to threefold that of α form PVDF crystal, with a small mismatch of 2.4% [eq. (4)]. Therefore, these results also confirm the epitaxial nucleation mechanism:

$$d_{\mathrm{PBA}}\,\% = \left|\frac{1.420 - 3\times 0.462}{1.420}\right| \times 100\% = 2.4\% \qquad (4)$$

CONCLUSION

In this research, effect of PVDF polymorphic structures on the crystallization behavior of PBS is systematically studied. The DSC and microscopic results show that β PVDF can improve T_c of PBS during the crystallization process with a cooling rate of 10°C/min, the T_c value can reach 86.9°C when PVDF content is 10 wt %. Further increase of PVDF content might lead to the decrease of T_c because of the dilutive effect. While α PVDF shows no accelerating effect on PBS crystallization. Both crystallization time span and spherulitic size of PBS decrease obviously with addition of β PVDF, because β PVDF enhances the primary nucleation of PBS by epitaxy mechanism. And a possible hydrogen bond interaction between β PVDF crystal and PBS chain is suggested.

ACKNOWLEDGMENTS

This work was supported by the National Natural Science Foundation of China (Grant No. 21304108) and the Science Foundation of China University of Petroleum–Beijing (No. YJRC-2013-14, 2462013BJRC001).

REFERENCES

1. Qiu, Z.; Komura, M.; Ikehara, T.; Nishi, T. *Polymer* **2003**, *44*, 7781.
2. Qiu, Z.; Ikehara, T.; Nishi, T. *Polymer* **2003**, *44*, 2799.
3. Ikehara, T.; Kimura, H.; Qiu, Z. *Macromolecules* **2005**, *38*, 5104.
4. Ikehara, T.; Kurihara, H.; Qiu, Z.; Nishi, T. *Macromolecules* **2007**, *40*, 8726.
5. He, Y.; Zhu, B.; Kai, W.; Inoue, Y. *Macromolecules* **2004**, *37*, 3337.
6. Wang, H.; Schultz, J. M.; Yan, S. *Polymer* **2007**, *48*, 3530.
7. He, Z.; Liang, Y.; Han, C. C. *Macromolecules* **2013**, *46*, 8264.
8. Pan, P.; Zhao, L.; Yang, J.; Inoue, Y. *Macromol. Mater. Eng.* **2013**, *298*, 201.
9. Wang, T.; Wang, H.; Li, H.; Gan, Z.; Yan, S. *Phys. Chem. Chem. Phys.* **2009**, *11*, 1619.
10. Lee, J. -C.; Tazawa, H.; Ikehara, T.; Nishi, T. *Polym. J.* **1998**, *30*, 327.
11. Li, Y.; Kaito, A.; Horiuchi, S. *Macromolecules* **2004**, *37*, 2119.
12. Qiu, Z.; Yan, C.; Lu, J.; Yang, W.; Ikehara, T.; Nishi, T. *J. Phys. Chem. B* **2007**, *111*, 2783.
13. Qiu, Z.; Yan, C.; Lu, J.; Yang, W. *Macromolecules* **2007**, *40*, 5047.
14. Wang, T.; Li, H.; Wang, F.; Yan, S.; Schultz, J. M. *J. Phys. Chem. B* **2011**, *115*, 7814.
15. Wang, T.; Li, H.; Wang, F.; Schultz, J. M.; Yan, S. *Polym. Chem.* **2011**, *2*, 1688.
16. Penning, J. P.; John Manley, R. St. *Macromolecules* **1996**, *29*, 84.
17. Liu, L. -Z.; Chu, B.; Penning, J. P.; John Manley, R. St. *Macromolecules* **1997**, *30*, 4398.
18. Isayeva, I.; Kyu, T.; John Manley, R. St. *Polymer* **1998**, *39*, 4599.
19. Yang, J.; Pan, P.; Hua, L.; Zhu, B.; Dong, T.; Inoue, Y. *Macromolecules* **2010**, *43*, 8610.
20. Yang, J.; Pan, P.; Hua, L.; Feng, X.; Yue, J.; Ge, Y.; Inoue Y. *J. Phys. Chem. B* **2012**, *116*, 1265.
21. Nakafuku, C.; Sakoda, M. *Polym. J.* **1993**, *25*, 909.

22. Lai, W. -C.; Liau, W. -B.; Lin, T. -S. *Polymer* **2004**, *45*, 3070.
23. Lin, J. -H.; Woo, E. M. *Polymer* **2006**, *47*, 6826.
24. Lovinger, A. J. *J. Polym. Sci. Polym. Phys. Ed.* **1980**, *18*, 793.
25. Lovinger, A. J.; Keith, H. D. *Macromolecules* **1979**, *12*, 919.
26. Gregorio, R., Jr.; Cestari, M. *J. Polym. Sci. Polym. Phys.* **1994**, *32*, 859.
27. Gregorio, R., Jr. *J. Appl. Polym. Sci.* **2006**, *100*, 3272.
28. Gregorio, R. Jr; Borges, D. S. *Polymer* **2008**, *49*, 4009.
29. Ma, W.; Zhang, J.; Wang, X. *J. Mater. Sci.* **2008**, *43*, 398.
30. Lovinger, A. J. *Polymer* **1981**, *22*, 412.
31. Wang, J.; Li, H.; Liu, J.; Duan, Y.; Jiang, S.; Yan, S. *J. Am. Chem. Sci.* **2003**, *125*, 1496.
32. Ueberschlag, P. *Sensor Rev.* **2001**, *21*, 118.
33. Xu, J.; Guo, B. -H. *Biotechnol. J.* **2010**, *5*, 1149.
34. Ye, H. -M.; Tang, Y. -R.; Xu, J.; Guo, B. -H. *Ind. Eng. Chem. Res.* **2013**, *52*, 10682.
35. Ye, H. -M.; Wang, R. -D.; Liu, J.; Xu, J.; Guo, B. -H. *Macromolecules* **2012**, *42*, 5667.
36. Supaphol, P.; Harnsiri, W. H.; Junkasem, J. *J. Appl. Polym. Sci.* **2004**, *92*, 201.
37. Supaphol, P.; Thanomkiat, P.; Junkasem, J.; Dangtungee, R. *Polym. Test.* **2007**, *26*, 20.
38. Yasuniwa, M.; Iura, K.; Dan, Y. *Polymer* **2007**, *48*, 5398.
39. Zhu, P.; Ma, D. *Eur. Polym. J.* **1997**, *33*, 1817.
40. Lorenzo, A. T.; Arnal, M. L.; Albuerne, J.; Müller, A. J. *Polym. Test.* **2007**, *26*, 222.
41. Avrami, M. *J. Chem. Phys.* **1939**, *7*, 1103.
42. Avrami, M. *J. Chem. Phys.* **1940**, *8*, 212.
43. Avrami, M. *J. Chem. Phys.* **1941**, *9*, 177.
44. Legras, R.; Mercier, J. P.; Nield, E. *Nature* **1983**, *304*, 432.
45. Wittmann, J. C.; Lotz, B. *J. Polym. Sci. Polym. Phys. Ed.* **1981**, *19*, 1837.
46. Ihn, K. J.; Yoo, E. S.; Im, S. S. *Macromolecules* **1995**, *28*, 2460.
47. Kobayashi, M.; Tashiro, K.; Tadokoro, H. *Macromolecules* **1975**, *8*, 158.
48. Cha, B. J.; Yang, J. M. *J. Membrane Sci.* **2007**, *291*, 191.
49. Nikolic, M.; Djonlagic, J. *Polym. Degrad. Stabil.* **2001**, *74*, 263.
50. Iwata, T.; Kobayashi, S.; Tabata, K.; Yonezawa, N.; Doi, Y. *Macromol. Biosci.* **2004**, *4*, 296.